

Spatially resolved height response of phase-shifting interferometers measured using a patterned mirror with varying spatial frequency

Jiyoung Chu

National Institute of Standards and Technology
Manufacturing Engineering Laboratory
100 Bureau Drive
Gaithersburg, Maryland 20899-8223
and
Samsung Electronics Company
416, Maetan 3-dong, Yeongtong-gu
Suwon-si, Gyeonggi-do, South Korea

Quandou Wang

National Institute of Standards and Technology
Manufacturing Engineering Laboratory
100 Bureau Drive
Gaithersburg, Maryland 20899-8223

John P. Lehan, MEMBER SPIE

University of Maryland Baltimore County
Department of Physics
1000 Hilltop Circle
Baltimore, Maryland 21250
and
NASA Goddard Space Flight Center
8800 Greenbelt Road
Greenbelt, Maryland 20771

Guangjun Gao, MEMBER SPIE

National Institute of Standards and Technology
Manufacturing Engineering Laboratory
100 Bureau Drive
Gaithersburg, Maryland 20899-8223
and
National University of Singapore
Division of Bioengineering
7 Engineering Drive 1, Block E3A #04-15
Singapore 117574, Singapore

Ulf Griesmann

National Institute of Standards and Technology
Manufacturing Engineering Laboratory
100 Bureau Drive
Gaithersburg, Maryland 20899-8223
E-mail: ulf.griesmann@nist.gov

1 Introduction

Phase-shifting interferometers are widely used instruments for measuring form errors of precision surfaces. The performance of interferometers depends on the optical system

Abstract. In the performance evaluation of phase-shifting interferometers for figure metrology, the height response, or height transfer function, is rarely taken into consideration, because in most applications smooth surfaces are measured and only the lowest spatial frequencies are of interest. For measurements with low uncertainty it is important to understand the height response as a function of the spatial-frequency content of a surface under test, in particular when it contains form-error components with frequencies at the high end of an interferometer's spatial-frequency passband. A mirror with a patterned area of 140-mm diameter, consisting of several subpatterns with varying spatial frequency, was used to evaluate the spectral response. Our goal was to develop a method for efficient mapping of the spectral response over the circular field of view of a phase-shifting interferometer. A new way of representing the dependence of the spectral response on the field of view of an interferometer is described. © 2010 Society of Photo-Optical Instrumentation Engineers. [DOI: 10.1117/1.3488052]

Subject terms: interferometry; spatial frequency; height response.

Paper 090957PRR received Dec. 1, 2009; revised manuscript received Jul. 23, 2010; accepted for publication Jul. 27, 2010; published online Sep. 20, 2010.

design, the quality of optical components, uncertainties due to phase-shifting algorithms and phase unwrapping, environmental conditions, and so on. Most precision optical surfaces have form errors with spatial frequencies much below 1 cycle/mm, and the transfer function of an interferometer at higher spatial frequencies is usually irrelevant in

evaluating the form errors of an optical surface that affect imaging performance. However, form errors in the mid and high spatial-frequency ranges result in scattered light and thereby reduce the performance of optical systems. (The boundary of the mid spatial-frequency range is commonly set at 0.5 mm^{-1} .) In high-end optical systems, higher-frequency form errors must be characterized accurately, and it is important to determine the response of interferometers for all spatial frequencies the instrument was designed to measure.

The most direct way of measuring the response of an interferometer at different spatial frequencies is to create sinusoidal phase profiles having different spatial frequencies. This can be done, for example, by using the interference between flats to generate an effective phase grating in the way described by Novak et al.^{1,2} Alternatively, sinusoidal surfaces can be used to measure the spectral response of an interferometer, as was done by Bouillet and Daurios,³ an approach that has the advantage of conceptual purity. However, sinusoidal surfaces present a formidable fabrication challenge, and it is difficult to create surfaces that are purely sinusoidal. In contrast, rectangular profiles can be made easily and very accurately with modern lithographic technology, which can outweigh the disadvantage that rectangular profiles contain a complicated spectrum of spatial frequencies. Mirrors with a step profile were used by Novak et al.² to corroborate the spectral transfer functions measured with the effective phase grating. A similar step object was also used by de Groot and de Lega⁴ to measure the transfer function of an interferometric microscope system. Dörband and Hetzler⁵ have used a set of periodic patterns to measure the ratio of measured to real heights and thus to determine the spectral response of a phase-shifting interferometer.

A recently introduced approach to characterizing the spectral response of interferometers relies on the use of one- and two-dimensional pseudorandom gratings, which was described by Yashchuk et al.⁶ and Barber et al.⁷ Pseudorandom gratings with rectangular height profiles have uniform power spectral density, and the spectral response of the interferometer can be calculated from the power spectral density of the pseudorandom grating as measured by the interferometer.

Our chief motivation for the work described in this paper was to develop an efficient method for mapping the spectral response of a phase-shifting interferometer with spatial resolution in the field of view. Practitioners of interferometry undoubtedly know that it is often impossible to achieve perfect focus for the entire field. Uneven focus, and other reasons, result in uneven spectral response of the interferometer. Since our goal was to map the spatial-frequency response of a phase-shifting interferometer over its circular field of view, we designed a mirror with several types of arcuate patterns, of constant height and varying frequency, oriented radially. The mapping of the spectral response is achieved by clocking the mirror between measurements so that every type of pattern is measured in every segment of the field (see Sec. 2 for details).

With any method of measuring the spectral response of an interferometer using an artifact, one has to contend with the problem that the optical systems of interferometers and their detectors have different symmetry. The optical sys-

tems of interferometers commonly have rotational symmetry about an optical axis, at least approximately, while the properties of detectors are best described in a rectangular coordinate system. The mirror described in this paper is very well suited for evaluating the optical transfer function of an interferometer imaging system; it is not optimal for the evaluation of the detector transfer function, because fundamental detector properties such as the sampling period in the radial direction are angle-dependent.

We describe the use of the mirror for mapping the spectral response of two different interferometers and suggest ways of presenting the variability of the spectral response. Preliminary results and details of the mirror fabrication were described by Chu et al.⁸

2 Mirror Design and Fabrication

We fabricated a patterned mirror that allowed us to test the height response of interferometers with apertures of 150 mm as a function of spatial frequency. The mirror was fabricated on a substrate with 150 mm diameter, because a substrate with this diameter was easily obtained. Since the substrate could not be patterned near the edge, the entire pattern is contained within a circle of 140 mm diameter, which implies that the interferometer transfer functions could be tested only in a circular area of 140 mm diameter, regardless of the actual apertures of the interferometers. The pattern is divided into twelve equal-angle fan-shaped sections as shown in Fig. 1(a). Each section consists of arc segments with varying line width in the radial direction. The arc segments in each subpattern are connected to avoid problems with phase unwrapping in the phase-shifting interferometer. All sections have a nominal height of 100 nm. The connector strip and the gaps between the sections can be considered reference surfaces for the top and bottom of the subpatterns except near the center of the mirror, where the strip is too narrow for an interferometric height measurement. Near the center, the interferometric height measurements had to be augmented with profilometer measurements.

There are three subpatterns, having different spatial-frequency distributions. Subpattern 1 has high spatial frequencies at intermediate radii and low frequencies near the center and the edge of the mirror. Subpatterns 2 and 3 have decreasing and increasing spatial frequencies in the radial direction, respectively. The profiles of the three patterns are depicted in Fig. 1(b). The spatial frequency in the subpatterns is designed to be distributed evenly between 0.133 and 1 cycle/mm, and the width of the arc segments ranges from 0.5 to 3.75 mm, as shown in Fig. 1(c). The three different subpatterns cover a quadrant of the circle and are inserted four times to fill the whole area. This seemingly peculiar pattern distribution has some advantages. The height transfer function can be measured, at least coarsely, at all aperture locations for all spatial frequencies by making three measurements between which the patterned mirror is rotated by 30 deg. In addition, a flat substrate for patterning usually has surface variations primarily along the radial direction, and the pattern distribution makes it easy to measure and compare height profiles along the radial direction.

The patterned mirror was fabricated at the NanoFab of the Center for Nanoscale Science and Technology (CNST)

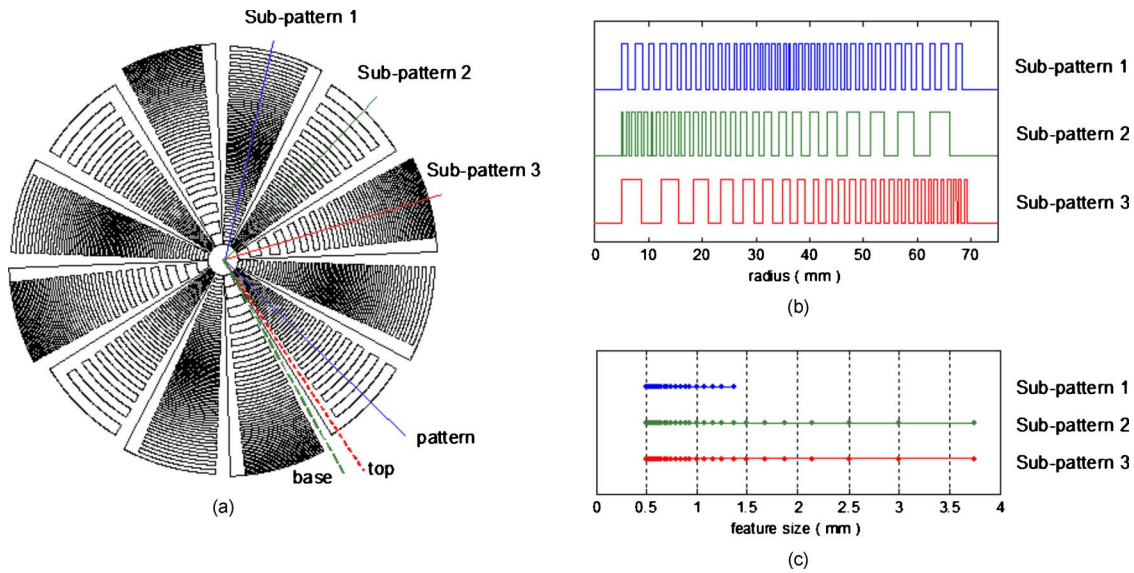


Fig. 1 (a) Pattern with varying spatial-frequency content, (b) profiles of the three subpatterns, (c) range of feature sizes (line widths) in the subpatterns.

at the National Institute of Standards and Technology (NIST). A photolithography process was employed to create a rectangular relief pattern on a substrate. To prevent the effects of temperature fluctuation and deformation of the substrate, a fused silica substrate of 20 mm thickness was used. The diameter of the substrate is 150 mm, because that was the largest substrate that could be patterned with the tools at the NanoFab. Many phase-shifting interferometers in the field, which are used for figure metrology, have 150 mm apertures. The peak-to-valley flatness error of the substrate is approximately 150 nm ($\lambda/4$ at 632.8 nm). The photomask for the lithography was made by a commercial photomask company.

The substrate was first coated with a 100 nm-thick chromium layer using a sputter deposition process. Then, a positive photoresist was spin-coated on the chromium layer and patterned using the photomask in a mask aligner. After wet etching, a chromium layer of 50 nm thickness was deposited to make the whole mirror uniformly reflective. The pattern height is very close to 100 nm. This height was chosen to ensure that the optical path difference between high and low areas of the mirror remains below $\lambda/2$ for the

632.8 nm wavelength of the phase-shifting interferometers. The pattern height uniformity was measured with a stylus profilometer. The pattern heights were found to be within 5% of the nominal height of 100 nm for the entire mirror area.

3 Height Transfer Function

The fabricated mirror was measured with a 150 mm aperture phase-shifting interferometer and, for comparison, with NIST's Extremely Accurate Calibration Interferometer (XCALIBIR).⁹ XCALIBIR is a high-accuracy Fizeau interferometer capable of measuring flats up to 300 mm diameter. A schematic layout of the interferometer is shown in Fig. 2(a). XCALIBIR can be configured with imaging lenses having different focal lengths to control the image size on its charge-coupled device (CCD) camera (1024 × 1024 pixels). Imaging lenses with focal length $f=200$, 125, and 100 mm were chosen for measurements. The images of the mirror on the CCD camera have resolutions of about 0.208, 0.333, and 0.415 mm/pixel, respectively. For most of these configurations the diameter of the interferom-

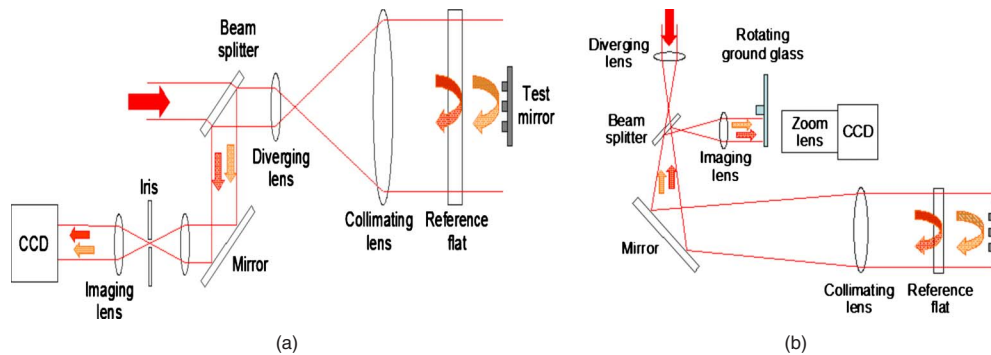


Fig. 2 Schematic diagram of (a) XCALIBIR, (b) a Fizeau interferometer with 150-mm aperture.

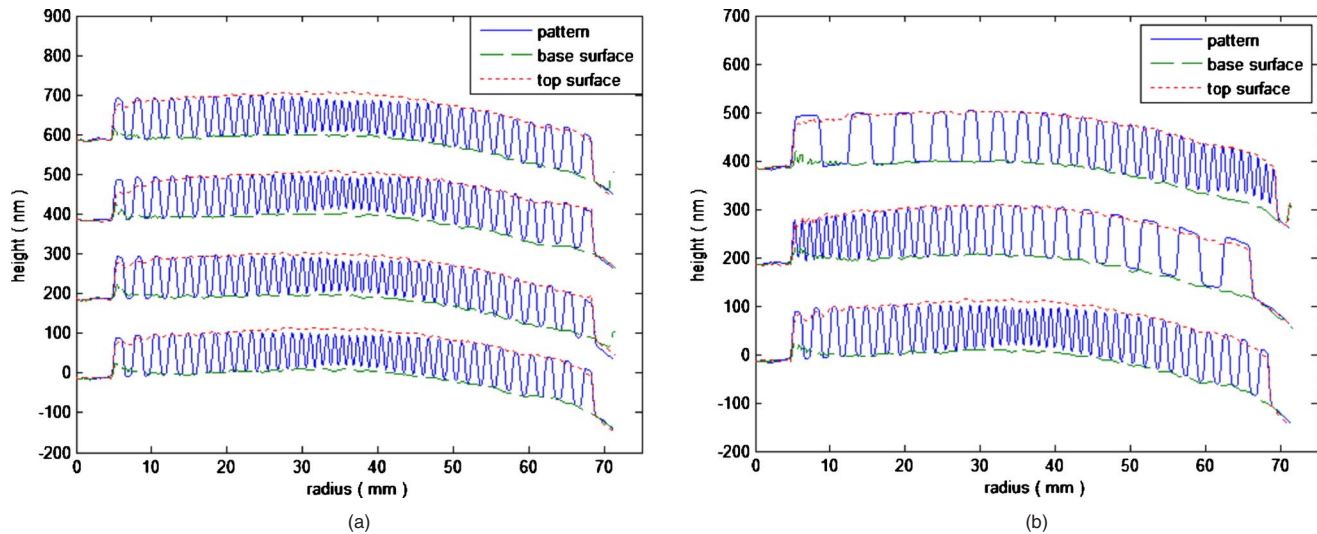


Fig. 3 The height profiles measured with XCALIBIR using an image resolution of 0.333 mm/pixel. (a) Height profiles of subpattern 1 in radial direction for four different azimuths separated by 90 deg. (b) Radial height profiles of the three subpatterns in one quadrant.

eter's field of view is larger than 140 mm and the spectral response of the interferometer was only measured for the middle of the field. The interferometer with 150 mm aperture is also a Fizeau interferometer. It has the layout shown in Fig. 2(b). Unlike the imaging system of XCALIBIR, the interferometer has an imaging system that is not fully coherent. The interferometer images the part under test onto a rotating ground-glass screen with fixed magnification. The image on the screen is then reimaged onto the CCD detector (1007×1007 pixels) using a zoom lens. In our measurements the images have a resolution of approximately 0.157 mm/pixel. The rotating ground glass in the imaging plane reduces the spatial coherence of the beams to prevent interference by stray reflections in the zoom lens, at the expense of blurring the image and the potential to introduce vibration noise.^{10,11}

The mirror was measured with both interferometers, centered on the optical axis at best focus. The measured pattern sizes range from 3.003 to 22.523 pixels/cycle for XCALIBIR with the imaging lens of $f=125$ mm, and 6.369 to 47.771 pixels/cycle for the other interferometer. Both interferometers have sampling resolutions that are sufficiently high to measure the pattern. The sampling resolution of the interferometer with 150 mm aperture is about twice that of XCALIBIR. The full images on the CCD cameras by XCALIBIR with the $f=125$ mm imaging lens and the interferometer with the smaller aperture correspond to flats 300 and 150 mm in diameter, respectively. Figures 3 and 4 show the height profiles measured by both interferometers. The blue solid line represents the pattern profile, and the red dotted and green dashed lines are the top profile of the connector strip and the bottom profile of the gap next to the connector strip. These three profiles are located as indicated in Fig. 1.

One difficulty in analyzing the measurement data is that, on one hand, the imaging systems of interferometers usually have an optical axis and their properties are at least nominally rotation-invariant and best described in polar co-

ordinates. The detector, on the other hand, samples the image in the focal plane on a square grid. Radial profiles, as discussed here, must be calculated from the sampled data through interpolation unless they happen to follow a horizontal or vertical pixel line. Each radial profile in Figs. 3 and 4 is the average of five closely spaced profiles with 0.5 deg angular separation, to improve the signal-to-noise ratio. Points on the lines are spaced at 0.25 pixel, and the corresponding height values were determined using linear interpolation based on the four pixels nearest to the interpolation point. The nearest-neighbor interpolation introduces the least amount of filtering in the interpolated data.

The standard deviations of the interpolated profiles can be taken as a measure of the uncertainty of the height measurements. For the profiles obtained from measurements with XCALIBIR, the mean of the uncertainties of the profile heights (1σ) is 2.5 nm. For the smaller interferometer the mean uncertainty of the height measurements is 1.4 nm. Top and bottom profiles in Fig. 3(b) near the center of the mirror do not show the true profile, because the image resolution is insufficient to correctly image these narrow areas. Higher-resolution images confirm that the height of these profiles is the same at all radii.

Figure 3(a) shows the height profiles measured with XCALIBIR for subpattern 1 along the radial direction for four different azimuths separated by 90 deg. All pattern profiles are located inside the red and green lines, and the pattern heights decrease identically at high spatial frequencies, regardless of the azimuth. For subpatterns 2 and 3, the results are similar, suggesting that XCALIBIR has the same height transfer function regardless of direction. Figure 3(b) represents the measured radial height profiles of the three subpatterns in the first quadrant. The height changes of the three subpatterns for spatial frequency are almost identical, regardless of the radial position of the high spatial frequency, which indicates that the height transfer function of XCALIBIR is independent of the radial position for the area with 140 mm diameter around the optical axis that

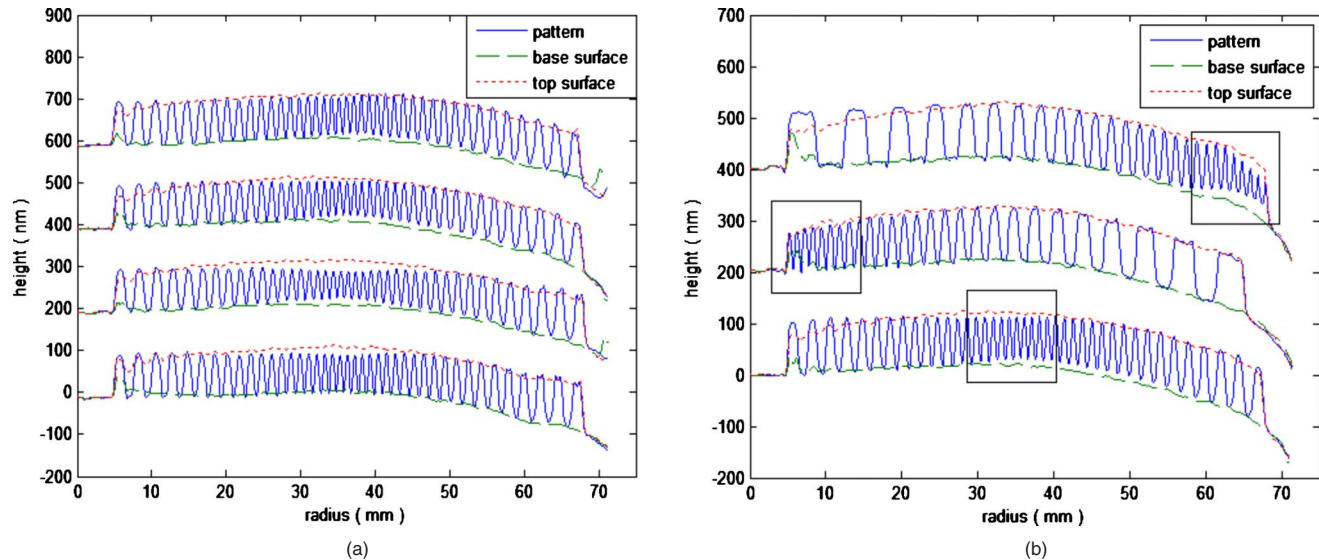


Fig. 4 The height profiles measured with the 150-mm-aperture interferometer using an image resolution of 0.157 mm/pixel. (a) Height profiles of subpattern 1 in radial direction for four different azimuths separated by 90 deg. (b) Radial height profiles of the three subpatterns in one quadrant.

could be measured with this mirror. These results shown in Fig. 3 suggest that XCALIBIR has nearly uniform height transfer function.

The results obtained for the other interferometer were different. Figure 4(a) shows the measured height profiles of subpattern 1 in four different azimuthal directions. In high-spatial-frequency areas, some profiles are attenuated more, despite the higher spatial resolution of the camera in this interferometer. Figure 4(b) shows the attenuation of measured pattern heights in regions of high spatial frequency, which are outlined by black boxes. The attenuation is clearly different at different radii. The profiles shown in Fig. 4 suggest a nonuniform height response over the field of view of this interferometer.

Instead of the qualitative appraisal of the interferometer responses summarized in Figs. 3 and 4, we now seek a quantitative description of the height response in the fields of view of the interferometers. Following Dörband and Hetzler,⁵ the height ratio for a spatial frequency ν at a location in the field of view of the interferometer, $H(\rho, \theta, \nu)$, is defined as the ratio of the pattern height measured by the interferometer, $h(\rho, \theta, \nu)$, to the true height $h_0(\rho, \theta)$:

$$H(\rho, \theta, \nu) = \frac{h(\rho, \theta, \nu)}{h_0(\rho, \theta)}, \quad (1)$$

where ρ and θ are the radial and angular positions in the interferometer field of view. For the mirror shown in Fig. 1 the true pattern height can conveniently be measured with the interferometer, because it is the height of the radial strip connecting the arcs. The height ratio obtained for a central line of a segment along the radial direction is assumed to be a representative value for the whole arc segment area in the section. In the ratio, the pattern height is the height difference between the center of an arc segment and the averaged height of the two low areas next to it. Using the uncertainty for the height measurements just discussed, the uncertainty

for measurements of the height ratio function can be estimated from Eq. (1). For the XCALIBIR interferometer this uncertainty is 0.04, and for the smaller-aperture interferometer it is 0.02.

Figure 5 shows the height ratios as function of the spatial frequency, averaged for all twelve mirror segments in three orientations. The curves in Fig. 5 represent the average height ratio and its variability over the field of view. XCALIBIR was tested for three imaging lenses with $f = 200$ mm, $f = 125$ mm, and $f = 100$ mm. Figure 5(a) shows the height transfer function as a function of object spatial frequency in cycles per millimeter. The lower the detector resolution, the sooner the height ratio drops as a function of spatial frequency in XCALIBIR. With the $f = 200$ mm imaging lens (0.208 mm/pixel), the pattern height can be measured without significant height change regardless of spatial frequency. XCALIBIR with the imaging lens of $f = 125$ mm and the other interferometer have similar spectral response. The error bar at each point represents the standard deviation of the height ratios from all twelve sections. It represents the *variability* of the height ratio for a given spatial frequency over the field of view and should not be mistaken for the *uncertainty* of the height ratio. Figure 5(a) can be used to determine the maximum spatial frequency component of an object at which a height can be measured reliably without attenuation by the interferometer transfer function.

An interesting result, shown in Fig. 5(b), is obtained when the data in Fig. 5(a) are plotted against the number of cycles per pixel on the CCD detector. Curves in Fig. 5 were obtained at the best focus at the aperture center and change slightly with alignment. XCALIBIR and the other interferometer exhibit strikingly different height response curves in Fig. 5(b). The height response for XCALIBIR begins to drop at about 0.2 cycle/pixel, which is close to half the cutoff frequency of 0.5 cycle/pixel for the CCD image.

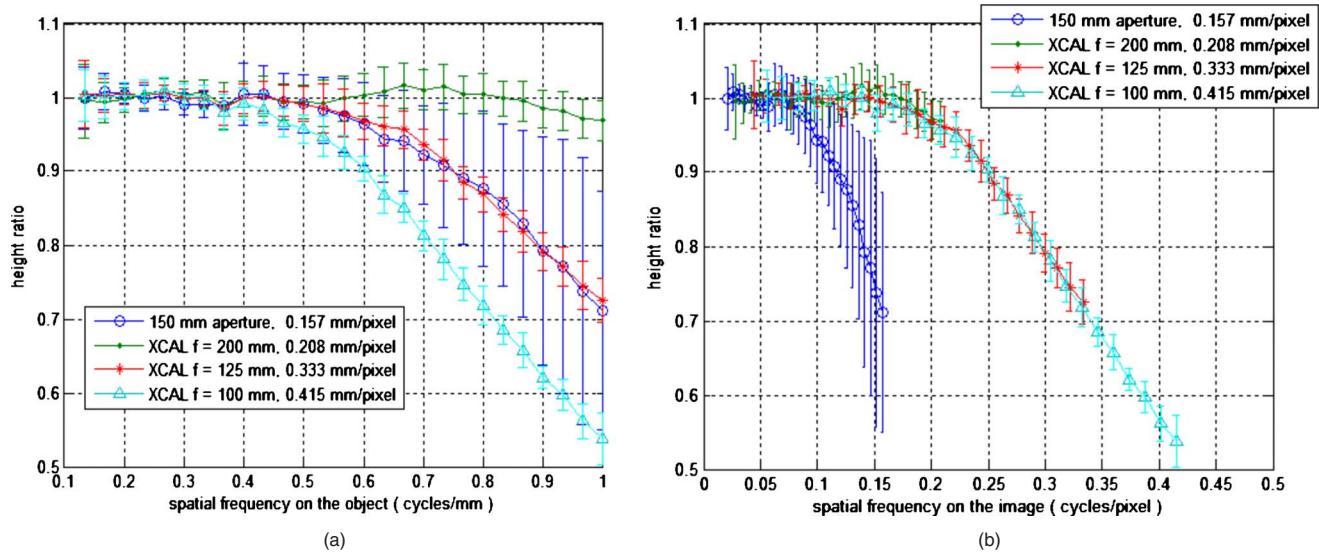


Fig. 5 Measured height ratios according to Eq. (1) for both interferometers at best focus at the aperture center: (a) as a function of the spatial frequency in object space, (b) as a function of the spatial frequency on the image. Error bars represent the variability of the height ratio over the field of view, not the uncertainty. The uncertainty (standard deviation) of the height ratio is 0.04 for XCALIBIR and 0.02 for the smaller-aperture interferometer.

This means that XCALIBIR has a height response curve that is mainly determined by the effective image resolution, which is set by the image magnification in the optical system and the pixel resolution of the CCD camera. For the other interferometer, the curve drops quickly, beginning at 0.08 cycle/pixel. In this case the effects of detector and imaging system are reversed. In this interferometer the imaging system contains a rotating ground-glass screen to reduce the degree of coherence of the laser beam, which inevitably results in some blurring of the image. In addition, the imaging system, including the zoom lens, may be less

well corrected than the imaging system of XCALIBIR and cause aberrations on the image. The consequence is that the response of the smaller-aperture interferometer to high spatial frequencies is limited by the imaging system, not by the detector. This conclusion is also supported by the variability of the height response over the field of view, which cannot be explained by the properties of the detector.

Figure 6 is an alternative depiction of the frequency response of the two interferometers. It shows the spatial cut-off frequency at which the height ratio drops below 0.9, which is denoted as $H_{0.9}$, for the 36 zones of the aperture

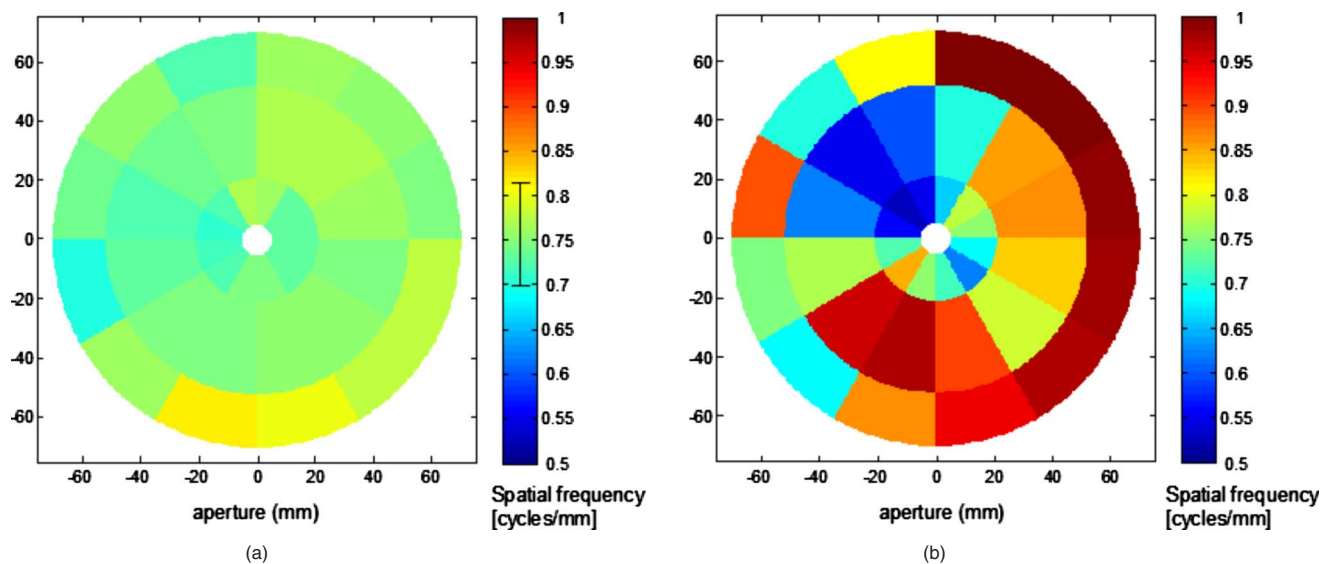


Fig. 6 The spatial cutoff frequency at the height ratio $H_{0.9}$ for (a) XCALIBIR (0.333 mm/pixel), (b) the comparison interferometer with 150 mm aperture (0.157 mm/pixel). The uncertainty (standard deviation) of the height ratio is 0.04 for XCALIBIR, indicated with an error bar, and 0.02 for the smaller-aperture interferometer.

that could be tested with the mirror. Since the patterned mirror has different spatial frequencies at radial and azimuthal positions, the height ratio at each zone of the aperture can be obtained by measuring the patterned mirror three times with 30 deg rotations around the center of the mirror in the same aperture. The XCALIBIR result with the $f=125$ mm imaging lens shows an almost uniform distribution of the spatial cutoff frequency within a range of 0.12 cycle/mm for $H_{0,9}$ in Fig. 6(a). The uncertainty of the mean of $H_{0,9}$, 0.04, is indicated with an error bar in Fig. 6(a). It shows that the variability of the cutoff frequencies $H_{0,9}$ remains within the measurement uncertainty. For the other interferometer in Fig. 6(b) the situation is very different. The variability of the cutoff frequencies $H_{0,9}$ far exceeds their uncertainty of 0.02. An asymmetry of the cutoff frequency is also clearly noticeable. In one half of the aperture, the cutoff frequency for $H_{0,9}$ tends to be significantly lower than in the other half.

4 Conclusions

In this paper, the height response of two different phase-shifting interferometers was compared using a mirror with a relief pattern of varying spatial frequency content. The patterns on the mirror were designed to facilitate efficient mapping of the variability of an interferometer response function in a circular area with 140 mm diameter. The height response for the XCALIBIR interferometer was uniform within the measurement uncertainty in the radial and azimuthal directions over the tested part of the aperture and started to decrease near half of the CCD cutoff frequency. A second interferometer, with 150 mm aperture, that we evaluated showed a very uneven height response distribution, and the height ratio dropped at frequencies far lower than half of the CCD cutoff frequency. The main reasons for the different characteristics are the properties of the different imaging systems. An important observation is that the instrument transfer function of an interferometer can be remarkably uneven over the field of view.

The patterned mirror that was designed for this investigation was found to have some disadvantages. While the mirror permits mapping of the interferometer response with only three measurements (see Fig. 6), the spatial resolution is coarse and the chirped frequency patterns complicate the data analysis. The variable frequency patterns are also unsuited to mapping the response of an interferometer with an aperture less than 140 mm. Better spatial resolution can be achieved with a set of fixed frequency patterns, albeit at the expense of having to make more measurements.

References

1. E. Novak, C. Ai, and J. C. Wyant, "Optical resolution of phase measurements of a laser Fizeau interferometer," *Proc. SPIE* **2870**, 545–552 (1996).
2. E. Novak, C. Ai, and J. C. Wyant, "Transfer function characterization of a laser Fizeau interferometer for high spatial frequency phase measurements," *Proc. SPIE* **3134**, 114–121 (1997).
3. S. Bouillet and J. Daurios, "Using phase objects to qualify the transfer function of Fizeau interferometers for high spatial frequencies," *Proc. SPIE* **6616**, 661628 (2007).
4. P. de Groot and X. C. de Lega, "Interpreting interferometric height measurements using the instrument transfer function," in *Proc. 5th Int. Workshop on Automatic Processing of Fringe Patterns*, pp. 30–

- 37, Springer, Berlin (2005).
5. B. Dörband and J. Hetzler, "Characterizing the lateral resolution of interferometers: the height transfer function of a phase shifting interferometer," *Proc. SPIE* **5878**, 587806 (2005).
6. V. V. Yashchuk, W. R. McKinney, and P. Z. Takacs, "Binary pseudo-random grating as a standard test surface for measurement of modulation transfer function of interferometric microscopes," *Proc. SPIE* **6704**, 670408 (2007).
7. S. K. Barber, P. Soldate, E. H. Anderson, R. Cambie, S. Marchesini, W. R. McKinney, P. Z. Takacs, D. L. Voronov, and V. V. Yashchuk, "Binary pseudo-random gratings and arrays for calibration of the modulation transfer function of surface profilometers: recent developments," *Proc. SPIE* **7448**, 744803 (2009).
8. J. Chu, Q. Wang, J. P. Lehan, G. Gao, and U. Griesmann, "Measuring the phase transfer function of a phase-shifting interferometer," *Proc. SPIE* **7064**, 70640C (2008).
9. U. Griesmann, Q. Wang, and J. A. Soons, "Three-flat tests including mounting-induced deformations," *Opt. Eng.* **46**, 093601 (2007).
10. R. G. Driggers, *Encyclopedia of Optical Engineering, Vol. 1*, Marcel Dekker, New York (2003).
11. E. P. Goodwin and J. C. Wyant, *Field Guide to Interferometric Optical Testing*, SPIE Press, Bellingham, WA (2006).

Jiyoung Chu is an optical engineer. She received her PhD from the Korean Advanced Institute of Science and Technology (KAIST) in 2006. She worked in National Institute of Standards and Technology, USA, as a guest researcher for three years and joined Samsung Electronics in 2009. Her research interests include interferometry and precision metrology.

Quandou Wang is an optical engineer with National Institute of Standards and Technology. He received his PhD from Changchun Institute of Optics, Fine Mechanics and Physics CIOMP, Chinese Academy of Sciences, in 2001. He was with CIOMP from 1992 to 2001. He was with Optical Science Center, University of Arizona, from 2001 to 2002, working on computercontrolled optical fabrication and testing of aspherical surfaces. His research interests include optical testing and precision metrology, optomechanics, optical instrument design, and fabrication of aspheric surfaces.

John P. Lehan received his BA in physics from Virginia Tech, and his Masters and PhD in optical sciences from the University of Arizona. He worked as an industrial researcher prior to coming to NASA Goddard in 2002, working on the Astro-E2 program. In 2004 he began working on the International X-ray Observatory in the role of metrology lead. His research interests include precision optical metrological methods, precision optical measurements, optical testing, optical design, precision optical manufacturing, and scatter from coated and uncoated surfaces.

Guangjun Gao received his BE in engineering in 2000 and his PhD in 2005 from Beijing Institute of Technology. He worked as a postdoc at National Astronomical Observatories of China NAOC, Chinese Academy of Science, from 2005 to 2007. He worked as a guest researcher at the National Institute of Standards and Technology until 2010 and the joined the Division of Bioengineering of the National University of Singapore. His research interests include optical design, optical metrology, diffractive optics, and optical microscopy.

Ulf Griesmann is a physicist with the National Institute of Standards and Technology. He received his Dr. rer. nat. from the University in Bonn, Germany, in 1992. He worked as a postdoc on atomic spectroscopy with short-wavelength lasers at Imperial College London, United Kingdom. After coming to NIST in 1994, he worked on precision spectrometry and properties of optical materials, and on interferometric surface form metrology since 2001. His current research interests include optical phase measuring interferometry, precision form metrology, methods for absolute metrology, metrology of free-form surfaces, and nano-structured optics.